Escola de Primavera de Transição e Turbulência
Blumenau 2020

ABCM Associação Brasileira de Engenharia e Ciências Mecânicas

12th Spring School on Transition and Turbulence
September 21st-25th, 2020, Blumenau, SC, Brazil

EPTT 2020-0113
NUMERICAL SIMULATION OF TURBULENT FLOWS IN DUCTS OPERATING UNDER INFESTATION OF MUSSELS

Fernando Oliveira de Andrade
Roberto Carlos Moro Filho
Universidade Tecnológica Federal do Paraná
fandrade@utfpr.edu.br
robertoc@utfpr.edu.br

Ada Scudelari
Universidade Federal do Rio Grande do Norte
ada@ct.ufrn.br

Abstract. *This work presents preliminary results of the use of a macroscopic model for numerical simulations of turbulent flows in ducts infested by mussels Limnoperna Fortunei. The computational model was based on the volumetric and temporal averages of the Navier-Stokes equations, in a way that the resulting model allowed simulations of turbulent flows in clean, porous and hybrid media. The averaged mass and momentum conservation equations were written for a representative elementary volume and discretized using the finite volume method, using a SIMPLE algorithm for the treatment of pressure-velocity coupling. A macroscopic $k-\varepsilon$ turbulence model was applied. Simulated results for mean velocity and turbulent kinetic energy distribution and head losses in infested ducts were obtained, discussed and compared to experimental measurements.*

Keywords: *Numerical simulations, turbulent flows in ducts, porous media, limnoperna fortunei.*

1. INTRODUCTION

In the last decades, several sectors of the industry have been affected by the presence of a specific type of mussel, considered exotic in Brazil, known as *Limnoperna Fortunei*. The extensive presence of this mussel in ducts have damaged components of water supply and irrigation systems. It has also been observed that the *Limnoperna Fortunei* tends to act in the obstruction of filters, in the obstruction of industrial and electric power generation equipment and in the damage of vessels engines (Mackie and Caludi, 2010; Diniz, 2010).

The *Limnoperna Fortunei* is original from the southeast Asia (Morton, 1976) and was first observed in Brazil in 1998, in the Jacuí River delta near Porto Alegre. With a dispersion rate of approximately 240 km/year (Darrigan and Drago, 2000; Darrigan, 2002), it reached five countries in South America: Argentina, Uruguay, Paraguay, Bolivia and Brazil, spreading to rivers, lakes and reservoirs (Darrigan and Bamborenea, 2005; Darrigan and Mansur, 2006; Darrigan and Bomborenea, 2009).

Significant damage associated with the presence of this mussel could be observed in water supply systems. Excessive clogging in ducts caused obstruction of filters and other components of water distribution systems, resulting in increasing pressure drop along the ducts. As highlighted by Martinez et al. (2012), the infestation of water lifting facilities by *Limnoperna Fortunei* represents a potential increase in water pumping costs. Once the infestation has started, the pressure drop coefficient values rise rapidly, resulting in a reduction in the pumped flows. This not only generates financial impact, but also an operational difficulty to adequately meet the population's water demand.

Recent studies have been developed to mitigate damages to the public water distribution network, focusing on evaluating the hydraulic characteristics in pressurized ducts with infestation by *Limnoperna Fortunei*. Most of the studies available are based on experimental observations of velocity and pressure fields, seeking to quantify the hydraulic and hydrodynamic changes imposed by infestation in the ducts (Resende et al., 2007; Polman et al., 2013; Resende, 2014).

In this context, the present work aimed to develop a computational model for simulating pressurized turbulent flows in ducts, with and without the presence of mussels. The developed model was based on the volumetric formulation of the two-dimensional steady-state averaged Navier-Stokes equations, using a classical $k-\varepsilon$ turbulence model. Numerical results were obtained to quantify incrustation influences on the velocity and pressure fields. Preliminary analysis of velocity and turbulent kinetic energy distributions, and head losses along the duct were performed, comparing simulated results with the experimental measurements of Resende et al. (2007) for different discharges.

2. MATHEMATICAL FORMULATION

The mathematical model used in this work is based on a macroscopic formulation of the mass and momentum conservation equations, considering the simplifications of Newtonian and incompressible fluid, two-dimensional and steady-state flow. The heuristic equation of momentum conservation can be found in some studies (Kaviany, 1995; Pedras, 2000) and corresponds to the Navier-Stokes equations, obtained by the process of temporal and volumetric averages of the flow variables. The main desirable characteristic of these equations is that they can be used in both clean and porous media.

Using the Reynolds decomposition and taking the temporal and volumetric averages, the mass and momentum conservation equations are given by, respectively:

$$\nabla \cdot \overline{\mathbf{u}}_D = 0 \tag{1}$$

$$\rho \nabla \cdot \left(\frac{\overline{\mathbf{u}}_D \overline{\mathbf{u}}_D}{\phi} \right) = -\nabla \left(\phi \left\langle \overline{p} \right\rangle^i \right) + \mu \nabla^2 \overline{\mathbf{u}}_D + \nabla \cdot \left(-\rho \phi \left\langle \overline{\mathbf{u}' \mathbf{u}'} \right\rangle^i \right) + \phi \rho \mathbf{g} - \left[\frac{\mu \phi}{K} \overline{\mathbf{u}}_D + \frac{C_F \phi \rho \left| \overline{\mathbf{u}}_D \right| \overline{\mathbf{u}}_D}{\sqrt{K}} \right] \tag{2}$$

where the superscript i indicates values of the liquid phase, $\langle \cdot \rangle$ is the volumetric average, the overbar is the temporal average and $|\cdot|$ refers to module values, $\mathbf{u}_D$ is the surface velocity vector, also known as Darcy's velocity, $\mathbf{g}$ is the gravity acceleration vector, p is the pressure, ρ is the density, μ is the dynamic viscosity of the fluid and ϕ is the porosity. The last two terms of equation 2 represent the Darcy-Forchheimer's contribution, where K is the permeability of the porous medium and $C_F = 0.55$ is a drag coefficient, also known as Forchheimer coefficient.

The averaging processes lead to the Reynolds stress term, $\nabla \cdot \left(-\rho \phi \left\langle \overline{\mathbf{u}' \mathbf{u}'} \right\rangle^i \right)$, which needs to be modeled. This work employed a turbulent viscosity approach, with the use of a macroscopic $k - \varepsilon$ model, where the turbulent viscosity is given by:

$$\mu_T = \rho C_\mu f_\mu \frac{\left\langle k \right\rangle^{i^2}}{\left\langle \varepsilon \right\rangle^i} \tag{3}$$

where μ_T is the turbulent viscosity, C_μ and f_μ are empirical constants of the model, k is the turbulent kinetic energy and ε is the turbulent kinetic energy dissipation rate.

In this model, transport equations for the turbulent kinetic energy and dissipation rate were formulated according to:

$$\rho \nabla \cdot \left(\overline{\mathbf{u}}_D \left\langle k \right\rangle^i \right) = \nabla \cdot \left[\left(\mu + \frac{\mu_T}{\sigma_k} \right) \nabla \left(\phi \left\langle k \right\rangle^i \right) \right] - \rho \left\langle \overline{\mathbf{u}' \mathbf{u}'} \right\rangle^i : \nabla \overline{\mathbf{u}}_D + C_k \rho \frac{\phi k \left| \overline{\mathbf{u}}_D \right|}{\sqrt{K}} - \rho \phi \left\langle \varepsilon \right\rangle^i \tag{4}$$

$$\begin{aligned} \rho \nabla \cdot \left(\overline{\mathbf{u}}_D \left\langle \varepsilon \right\rangle^i \right) = \nabla \cdot \left[\left(\mu + \frac{\mu_T}{\sigma_\varepsilon} \right) \nabla \left(\phi \left\langle \varepsilon \right\rangle^i \right) \right] + C_1 \left(-\rho \left\langle \overline{\mathbf{u}' \mathbf{u}'} \right\rangle^i : \nabla \overline{\mathbf{u}}_D \right) \frac{\left\langle \varepsilon \right\rangle^i}{\left\langle k \right\rangle^i} \\ + C_2 f_2 C_k \rho \frac{\phi \varepsilon \left| \overline{\mathbf{u}}_D \right|}{\sqrt{K}} - C_2 f_2 \rho \phi \frac{\left\langle \varepsilon \right\rangle^i}{\left\langle k \right\rangle^i} \end{aligned} \tag{5}$$

where σ_k, σ_ε, C_k, C_1, C_2 and f_2 are constants that are prescribed according to the work of Pedras (2000).

2.1 Numerical methods

The governing equations were discretized using the finite volume procedure (Patankar, 1980) with a boundary-fitted non-orthogonal coordinate system. Equations 1 to 5 were discretized considering a two-dimensional control volume involving clean and porous media. The interface was positioned to coincide with the border between two control volumes, thus generating only volumes of the totally porous or totally clean types. The equations were then solved in the clean and porous domains, considering adequate interface conditions.

The system of algebraic equations was solved through the semi-implicit procedure according to Stone (1968). The SIMPLE algorithm for the pressure-velocity coupling was adopted to correct both the pressure and the velocity fields. The process starts with the solution of the momentum equations. Then the velocity field is adjusted in order to satisfy the continuity principle. This adjustment is obtained by solving the pressure correction equation. A structured uniform mesh containing 620 x 20 control volumes in the longitudinal and transversal directions, respectively, was adopted in the simulations. All computations were performed on an Intel Xeon 3.40 GHz, 16GB. For all cases a relative convergence of 10^{-5} was specified. The grid effects on the solutions were examined by increasing the number of nodes and verifying the solutions until the results no longer changed in a specified tolerance.

3. RESULTS AND DISCUSSIONS

The computational domain used in the simulations consisted of a 3100 mm long duct with a 100 mm diameter. A two-dimensional computational mesh was employed, adopting as boundary conditions uniform velocity at the inlet, walls with no-slip conditions and atmospheric pressure and no velocity derivative at the outflow. To represent the infestation of the mussels and the resulting decrease of the duct effective diameter, a 20 mm layer of a porous media was positioned at the walls. The duct was considered long enough for the complete development of the turbulent flows. Simulations were performed for discharges ranging from 2 to 20 m^3/s resulting in Reynolds numbers from 6.4×10^6 to 2.5×10^7 based on the characteristic scales of the duct entrance. Figure 1 shows a detailed view of the computational mesh used in the simulations, indicating the position of the mussels layer and the symmetry plane at $r = 0$. This figure indicates only the first 10 cm out of the total duct length of 310 cm.

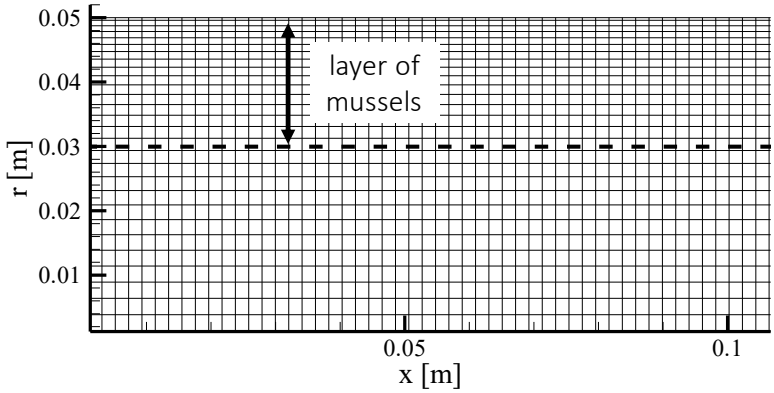

Figure 1. Detail view of the orthogonal mesh with 1502 x 30 elements, refined in the region closed to the wall. This figure shows 10 cm of a total length of 310 cm and a dashed line indicating the edge of the porous region.

An uniform value of $0.001\ cm^2$ was adopted for the permeability of the porous media and 0.45 for the porosity. These values were used in an attempt to simulate the presence of 0.5 mussel per cm^2 of duct, as indicated in the experiments performed by Resende et al. (2007). There is not an analytical relation between porosity and permeability, except for simple geometries, as a packed bed of spheres. Therefore, simulations treated the porous media as a packing of spheres. From the average dimensions of the mussels the authors defined the sphere diameters and calculated the porosity and permeability. The effects of porosity is subject of ongoing investigations and will be addressed in subsequent studies.

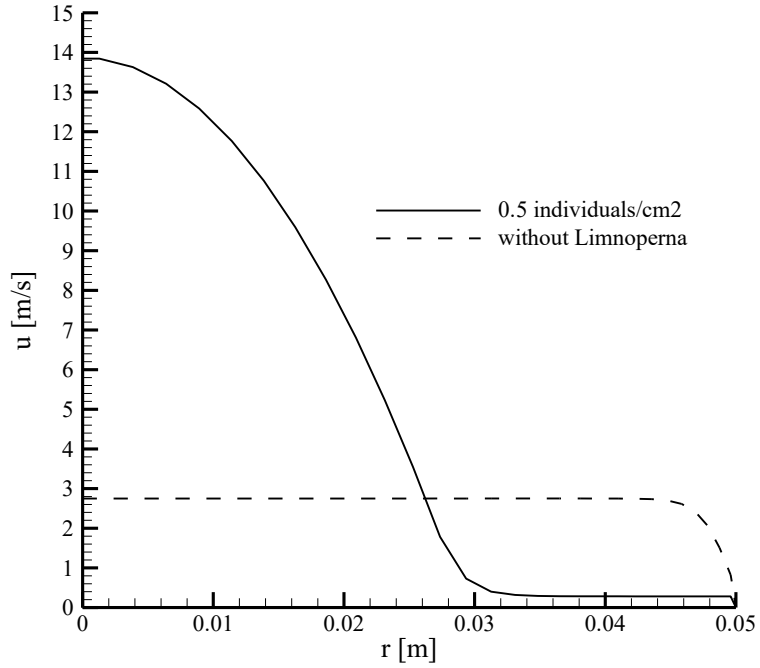

Figure 2. Comparison of the velocity profiles calculated at the pipe outlet ($x = 3.1\ m$) for cases with and without infestation considering a flow rate of $2.04\ m^3/s$.

Figure 2 shows the profiles of the streamwise component of velocity obtained through numerical simulations for cases without infestation and with infestation of 0.5 individuals per cm^2. This figure considers the symmetry of the distribution where the center of the pipe is located in $r = 0$. A typical exponential distribution for turbulent flow in pipes is observed in the absence of mussels. The layer of mussels near the pipe wall strongly influences the velocity distribution and makes the maximum velocity in the center of the pipe 5 times greater than the obtained value in the case without infestation.

Figure 3 shows profiles of turbulent kinetic energy at the outflow region of the pipe, considering a variation of the inflow velocity from 0.49 to 2.77 m/s with infestation of 0.5 individuals per cm^2. This figure also shows the profile of turbulent kinetic energy in a duct without infestation and inflow velocity of 2.24 m/s.

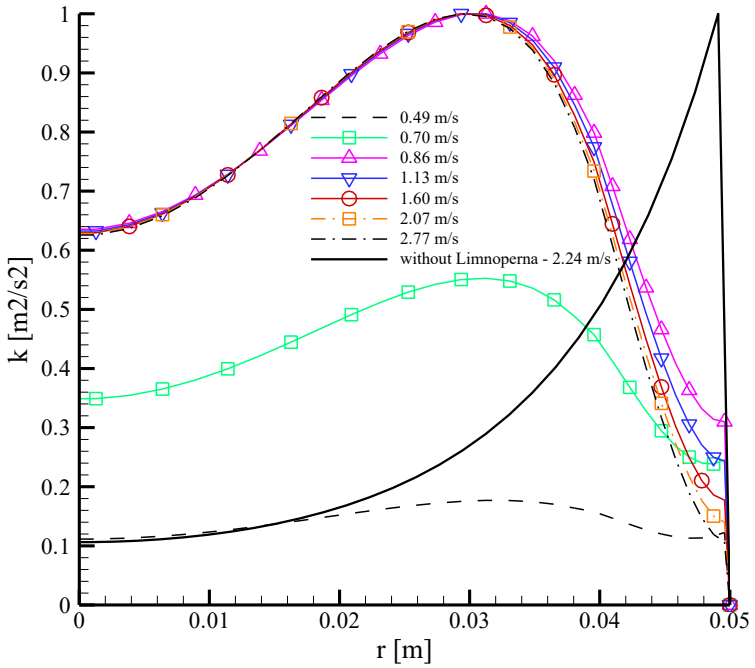

Figure 3. Comparison of the turbulent kinetic energy profiles calculated at the pipe outlet ($x = 3.1\ m$) considering different inflow velocities for cases with infestation of 0.5 individuals per cm^2 and without infestation.

Numerical results for the case of clean duct with inflow velocity of 2.24 m/s showed that the peak of the turbulent kinetic energy production occurs very near the wall, in the region of the largest velocity gradients. The values decay exponentially towards the center of the duct and reaches a minimum at $r = 0$. It can be observed a significant change of the distributions in the presence of mussels. For the lowest flow velocity of $0.49\ m/s$ an almost uniform distribution is observed. As the velocity increases to $0.70\ m/s$ the profile grows considerably and for velocities in the range of 0.86 to $2.77\ m/s$ the turbulent kinetic energy profiles collapse in a similar distribution.

It was observed for all cases a strong damping of the turbulent kinetic energy in the region of the mussels incrustation. The peak of turbulence production was shifted towards the center and positioned around $r = 0.03\ m$ for the velocity range of 0.86 to $2.77\ m/s$. When compared to the case of clean duct, the presence of mussels seemed to decrease the turbulence levels in the region close to the wall between $r = 0.04$ to $0.05\ m$ and to amplify the turbulent kinetic energy in the remaining cross section.

Figure 4 presents results of the numerical simulations of head losses per unity of length in ducts with and without infestation, and the comparisons with measured data of Resende et al. (2007). In the case of clean ducts, and for a flow of 7 m^3/s, the experiment showed head losses in the order of 0.003 m/m, whereas for 15 m^3/s this value increased to 0.02 m/m. Simulations results showed similar behaviors, with a lower offset of approximately 0.001 m/m.

In the presence of porous layer, and for a flow of 7 m^3/s, the measured head losses were approximately 0.2 m/m, while for 15 m^3/s this value was around 0.6 m/m. Simulation results underestimated the measured values by approximately 0.001 m/m. However, both measured data and simulation results showed that the presence of mussels on the duct increased the head losses by two orders of magnitude.

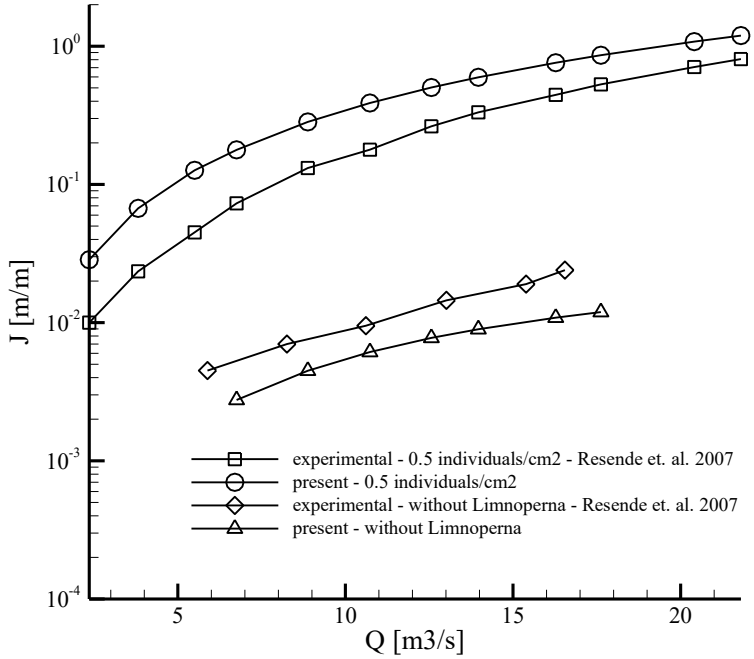

Figure 4. Head losses per unit of length as a function of the discharges. Comparison of simulated results with experimental measurements of Resende et al. (2007) for clean and infested ducts.

4. CONCLUSIONS

This work presented preliminary results of the use of a macroscopic model for numerical simulations of turbulent flows in ducts infested by the mussel Limnoperna Fortunei. The Reynolds average Navier-Stokes (RANS) equations with a $k - \varepsilon$ turbulence model were numerically solved for clean and porous media using the finite volume method.

Simulations showed that the cross-sectional velocity distribution was significantly affected by the presence of the mussels, such that the maximum velocity was amplified by a factor of five in the duct center. The distribution of turbulent kinetic energy was flattened in the region of the mussels incrustation and amplified in the remaining cross-section, when compared to the case of clean duct.

An analysis of head losses per unity of length with and without infestation was performed for different discharge levels, and simulated results were compared to measured data of Resende et al. (2007). Simulations managed to capture the overall behavior, showing that the presence of mussels drastically amplifies the head losses along the pipe flow. For a discharge of 10 m^3/s the head losses increased in one order of magnitude and this behavior tends to be even more intense for higher discharges. As a consequence, the preliminary results obtained from the simulations showed that the infestation of Limnoperna Fortunei impacts the hydraulic performance and increases the complexity of turbulent flows in ducts.

The developed numerical models were developed to be applied for general geometries in addition to the one studied experimentally. The numerical results obtained in this word added an analysis of turbulence which was not performed in the experiment of Resende et al. (2007).

5. ACKNOWLEDGEMENTS

The authors would like to thank the support received from the civil and environmental engineering department of the Federal Technological University of Paraná - UTFPR.

6. REFERENCES

Darrigan, G.A., 2002. “Potential impact of filter-feeding invaders on temperate inland freshwater environments”. *Biological Invasions*, Vol. 4, pp. 145–156.

Darrigan, G.A. and Bamborenea, C.A., 2005. “A bioinvasion history in south américa of limnoperna fortunei the gold mussel”. *American Malacologia Bullentin*, Vol. 20, p. 105.

Darrigan, G.A. and Bomborenea, C.A., 2009. *Introdução a Biologia das Invasões: biologia, dispersão, impacto, prevenção e controle*. Cubo Multimídia Ltda, São Carlos, SP, 1st edition.

Darrigan, G.A. and Drago, E., 2000. “Invasion of the exotic freshwater mussel limnoperna fortunei in south america”. *The Nautilus*, Vol. 114(2), pp. 69–73.

Darrigan, G.A. and Mansur, M.C.D., 2006. "Bio-invasión del mejillón dorado en el continenteamericano". *EDULP*, Vol. 1, pp. 93–110.

Diniz, D.M., 2010. *Avaliação da Influência Hidráulica da Infestação do Mexilhão Dourado nas Grades de Tomadas d'Água de Usinas Hidrelétricas*. Ph.D. thesis, Escola de Engenharia, Universidade Federal de Minas Gerais, Belo Horizonte, Brazil.

Kaviany, M., 1995. *Principles of Heat Transfer in Porous Media*. Springer New York, New York, USA, 1st edition.

Mackie, G.L. and Caludi, R., 2010. *Monitoring and control of macrofouling mollusks in fresh water systems*. CRC Press, Boca Raton, 2nd edition.

Martinez et al., 2012. "Impacto da infestação de limnoperna fortunei em bombas hidráulicas". In *Seminário de Estudos Avançados em Limnoperna fortunei*. Universidade Federal de Ouro Preto. Ouro Preto, Brazil.

Morton, S.B., 1976. "Control of limnoperna fortunei". *Journal of the Institution of Water Engineers and Scientists*, Vol. 30, pp. 147–156.

Patankar, S.V., 1980. *Numerical heat transfer and fluid flow*. Hemisphere New York, New York, USA, 1st edition.

Pedras, M.H.J., 2000. *Análise do Escoamento Turbulento em Meio Poroso Descontínuo*. Ph.D. thesis, Instituto Tecnológico de Aeronautica, São José dos Campos, Brasil.

Polman et al., 2013. "Impact of biofouling in intake pipes on the hydraulics and efficiency of pumping capacity". *Journal Desalination and Water Treatment*, Vol. 51, pp. 4–6.

Resende, M.F., 2014. *Interferências provocaads pela infestação de mexilhões dourados (Limnoperna fortunei) sobre bombas centrífugas e seu impacto em sistems de bombeamento de água*. Ph.D. thesis, Programa de Pós-graduação em engenharia mecânica. Universidade Federal de Minas Gerais, Belo Horizonte, Brasil.

Resende et al., 2007. "A variação das características hidráulicas em condutos forçados devido a infestação pelo limnoperna fortunei". In *XIX Seminário nacional de Produção e Transmissão de Energia Elétrica*. Rio de Janeiro, Brazil.

Stone, H.L., 1968. "Iterative solution of implicit approximations of multidimensional partial differential equations". *SIAM Journal on Numerical Analysis*, Vol. 5(3), p. 530–58.

7. RESPONSIBILITY NOTICE

The authors are the only responsible for the printed material included in this paper.